SWASH ZONE BASED REFLECTION DURING ENERGETIC WAVE CONDITIONS AT A DISSIPATIVE BEACH: TOWARD A WAVE-BY-WAVE APPROACH

Rafael Almar[1], Patricio Catalán[2], Raimundo Ibaceta[2], Chris Blenkinsopp[3], Rodrigo Cienfuegos[4], Mauricio Villagrán[4,5], Juan Carlos Aguilera[4] and Bruno Castelle[6]

This paper presents a 11-day experiment conducted at the high-energy dissipative beach of Mataquito, Maule Region, Chile. During the experiment, offshore significant wave height ranged 1-4 m, with persistent long period up to 18 s and oblique incidence. Wave energy reflection value ranged from 1 to 4 %, and results show that it is highly linked to both incoming wave characteristics and swash zone beach slope, and is well correlated to a swash-slope based Iribarren number. The swash acting as a low-pass filter in the reflection mechanism, our results show that the cut-off period is better determined by swash slope rather than incoming wave's period. A new low cost technique for observing high-frequency swash hydro-morphodynamics is introduced and validated using LIDAR measurements. A good agreement is found. Separation of uprush and backswash components using the Radon Transform illustrates the low-frequency filtering effect. These results show the key role played by swash mechanism in the reflection rate and frequency selection. More investigation is needed to describe the reflection process and its link with shoreface evolution, moving toward a swash-by-swash approach.

Keywords: Mataquito, Maule Region, Chile; beach reflection; incoming and outgoing wave separation; swash measurements technique; video; Lidar

INTRODUCTION

There is a potential for substantial wave reflection at the coast, depending on hydro- and morphodynamic conditions. Understanding the mechanisms at the origin of such reflection and the nature of reflected waves is crucial for various aspects of coastal science including energy balance, standing wave patterns and feedback with incoming waves, and resulting shoreface evolution. Pioneering studies based on laboratory experiments showed a link between reflection and the ratio of wave steepness to beach slope, hence vertical acceleration versus gravity, which can be summarized using the Iribarren number or surf-similarity parameter ξ (Iribarren and Nogales, 1949, see also Battjes et al., 1974). These studies considered monochromatic waves and planar slopes (e.g. Miche, 1951). However, field observations have shown that these predictions are weak for irregular waves and complex bathymetric profiles (Elgar et al., 1994). More recent studies, although mainly focused on engineering structure design (Sutherland 1998, among others), have underlined the key role played by swash zone dynamics, which controls the phase and energy of reflected waves. Because the measurement of reflection and swash is a difficult task in the field, observations are scarce.

On natural beaches, reflection values up to 0.6-0.8 have been observed. While this reflection rate attracted most of the attention, not many papers looked at reflection spectrum, which generally depends on swash slope more than incident waves (Mizuguchi, 1984; Miles and Russel, 2004). In this paper we investigate the energy reflection mechanism by linking offshore conditions and shoreface slope, moving toward a wave-by-wave approach. In the following sections, the instrumented study site and experiment are presented; results are given on bulk observation of reflection and on the application of a new technique of swash hydro-morphodynamics measurements. Finally, some concluding remarks are given on the potential of explaining reflection from swash-by-swash mechanisms and perspectives on beach equilibrium profiles are given.

DATA AND METHODS

Data used in this paper were collected at Mataquito beach (Fig. 1), Maule Region, 300 km south-west of Santiago de Chile, from November 30 to December 10, 2012. Mataquito is a micro-tidal, wave-dominated (H_s~2.4 m, T_p~12 s, South-West, Relative Tide Range *RTR*~0.6) environment. Sediment is medium grain-sized with *D50*=0.2 mm. The oblique energetic swell incidence drives a strong alongshore current and favoring a modal alongshore-uniform double-barred beach intermediate to dissipative profile (Iribarren number ξ<1; see Iribarren and Nogales, 1949). The beach suffered heavy

[1] LEGOS (IRD-CNRS-CNES-Univ. Toulouse), France
[2] Universidad Técnica Federico Santa María-CIGIDEN, Chile
[3] University of Bath, United Kingdom
[4] Pontificia Universidad Católica de Chile-CIGIDEN, Chile
[5] Universidad Católica de la Santísima Concepción, Chile
[6] EPOC (CNRS-Univ. Bordeaux), France

erosion after the 2010 Chilean tsunami, but recovered rapidly over the following year (Villagran et al., 2011).

Figure 1, Aerial photograph of Mataquito sandspit on Feb. 2 2012, looking south. Picture in small frame shows the state of the sandspit on April 2010, 2 months after the earthquake/tsunami that occurred on Feb. 27, 2010.

Figure 2, Swash hydro-morphodynamics measurements during the Mataquito dec 2013 experiment. a) LIDAR deployment on a scaffolding and b) optical video-poles setup.

This intensive experiment is the first of such importance to be conducted in Chile and involved about 30 researchers. An echosounder bathymetric survey of the whole area was conducted at the beginning of the experiment, during a period of uncommon low energy wave conditions (*Hs* of about 1.2 m). Beach survey was conducted daily using DGPS. Hydrodynamic wave and tide forcing were measured by an ADCP moored at a 10-m depth (900 m from the coastline). High frequency swash hydro and morphodynamics were measured (Fig. 2) using a LIDAR (Dec. 9th and 10th, see Blenkinsopp et al., 2010, Voudsoukas et al., 2014) mounted on a scaffolding and a new technique based on video-poles (see Results section for a description, or Ibaceta et al., 2014, this issue). 11 poles were deployed along a cross-shore profile within the swash zone and monitored by a full HD 30 Hz video camera. These high-frequency swash measurements were supported by a 2-camera permanent video system

(Cienfuegos et al., 2014), installed at the top a close hill, 100 m above MSL, which, using recent methods (Holman and Haller, 2013).

Fig. 3 shows the evolutions of wave, tide and beach slope over the experiment duration. Tide amplitude ranged from 0.4 to 1 m. A large swell hit the coast on Dec. 2, (H_s=4m, T_p=18 s, 10° incidence from shore-normal direction), followed by moderate energetic conditions starting on Dec. 5 (H_s=1-2 m, T_p=10-15s). During this period, accretive conditions induced an increase of mean shoreface slope. The swash zone slope (Fig. 3e), accounting for both tide level and intertidal shoreface profile, varied from 0.04 to 0.12 at the beginning of the observation period for a flat lower and steep upper beach, respectively, and evolved to a more intermediate constant slope (0.07) at the end of the observation period. Fig. 3f shows the Iribarren number ξ, defined as $\xi=tan(slope)/(H/L)^{0.5}$, H and L being offshore wave height and wavelength, the slope computed from swash slope (Fig. 3e). ξ varied from 1.5 to less than 0.5, following offshore wave steepness and beach slope evolution.

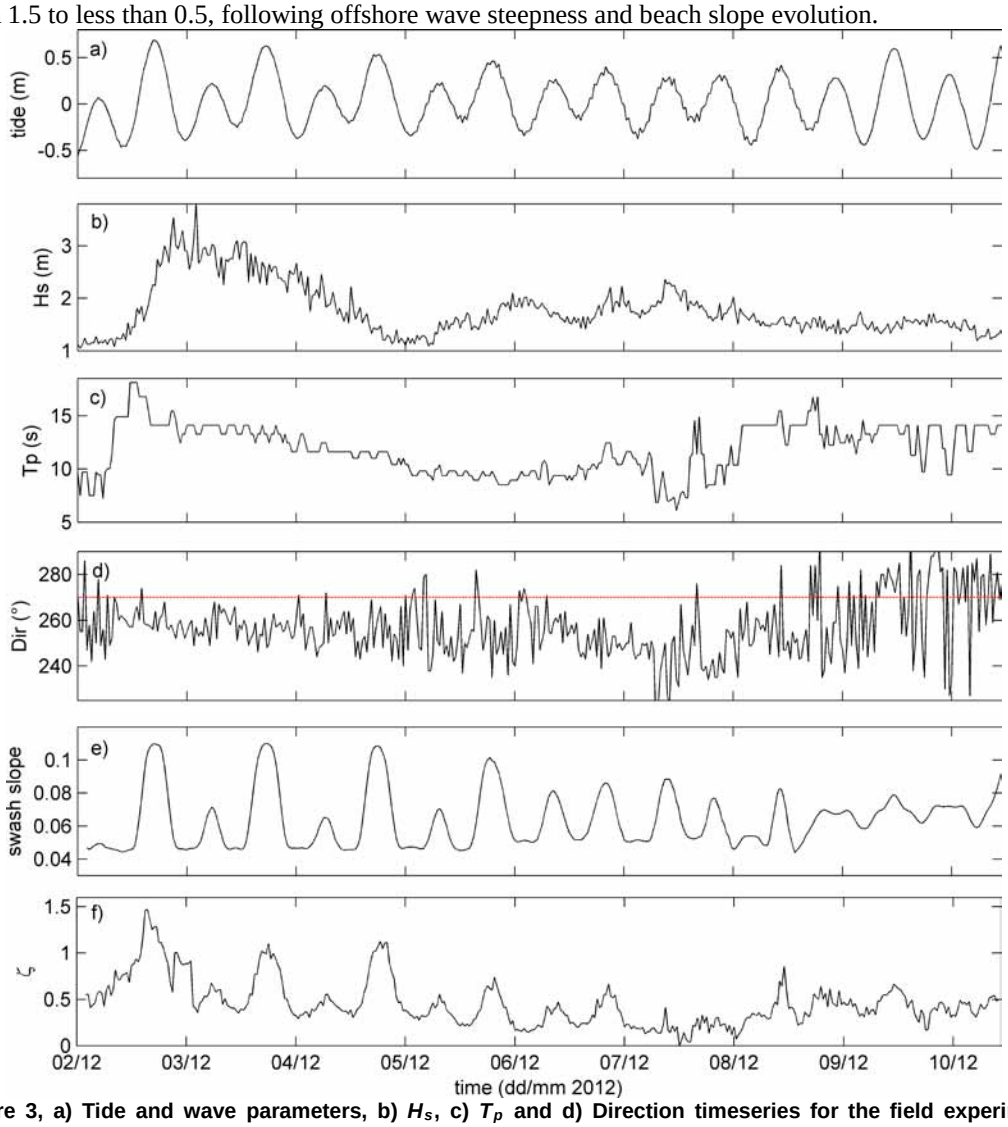

Figure 3, a) Tide and wave parameters, b) H_s, c) T_p and d) Direction timeseries for the field experiment conducted from Nov. 30 to Dec. 14 2013 at Mataquito sandspit, Maule Region, Chile. Red dashed line in d) stand for shore-normal direction. e) Swash zone slope, accounting for tidal level and beach profile. f) Iribarren number, defined as $\xi=tan(slope)/(H/L)^{0.5}$.

RESULTS AND DISCUSSION

Bulk reflection analysis from ADCP data

The separation of incoming and outgoing energy throughout the experiment was computed from the ADCP wave measurements. Fig. 4.a shows the timeseries of reflection, estimated every 40 min as the ratio of outgoing to incoming energy. Notice that here, contrary to some previous studies, the ratio

of energy instead of amplitude is considered (square value). Average reflection value is around 1%. The largest values (4%) are observed during the energetic swell that hit Mataquito on Dec. 3, after which they decrease rapidly and show some variability until the end of observation period. Following previous studies which suggest that the reflection coefficient is a function of the Iribarren number, we investigate the relationship between reflection and 3 hydro-and morphodynamics parameters: H_s, T_p, and swash zone slope (accounting for tidal level). A multilinear regression analysis was conducted between these parameters and reflection timeseries. The multilinear regression is defined as $Y=a_1X_1+a_2X_2+...a_nX_n$, where a_n are linear regression coefficients, X_n parameter timeseries and Y target timeseries to be explained. Relative variability explained by each component is given by $Var_n=Var(X_n)/Var(Y)$. The sum of all parameter contributions to the total variability can exceed 1 if parameters are not independent. Fig. 4.a, shows that a good agreement (R^2=0.74) is obtained between reconstructed and actual reflection. Wave and morphodynamic parameters contributed approximately equally to the reconstructed signal, accounting for 52 and 48%, respectively. This strongly supports the choice made by previous studies to use the Iribarren number which includes both beach slope and wave parameters to parameterize wave reflection. To examine this further, Fig. 5a shows wave reflection as a function of Iribarren number computed using the swash zone slope. An overall good fit is obtained (R^2=0.43), where E_{out}/E_{inc}=0.002*ξ. The commonly used $A_{out}/A_{inc}=0.1\ \xi^2$ (with reflection based on amplitude ratio, $0.01\xi^4$ for energy) formula developed by Battjes et al., (1974) slightly underestimates reflection (not shown). This has to be further investigated as it could be linked to an overestimation of the reflected component in the ADCP extraction due to wind waves generated by offshore winds.

Based on the assumption that the swash acts as a low-pass band filter (see Almar et al., 2012), we compute here the cut-off frequency of the reflected band; that is the highest frequency with substantial energy in the outgoing band. Fig. 4.b shows timeseries of cut-off period T_c which ranges between 8 and 33 s. A similar analysis is conducted to reconstruct T_c from waves and morphological parameters. Fig. 4.b shows that a good agreement (R^2=0.48) is found between reconstructed and actual T_c. Results also show that contrary to the findings for reflection, swash slope predominantly controls the reconstructed T_c value (72%), whereas wave parameters have only a secondary influence (27 %). This is in line with the previous observation that suggested the key role of swash slope on the reflected spectrum, though not it does no clearly quantify this link. These results motivated the development of a linear regression model for T_c only based on swash slope. Fig. 5.b shows the strong link (R^2=0.35) between T_c and slope, with T_c=32-191slope. Again, this result underlines the predominant role of swash hydro-morphodynamics on reflection and motivates further studies to investigate the reflection process within the swash zone. In the next section we introduce a recently developed method to measure swash-by-swash dynamics and use it to separate the incoming and reflected components of individual waves.

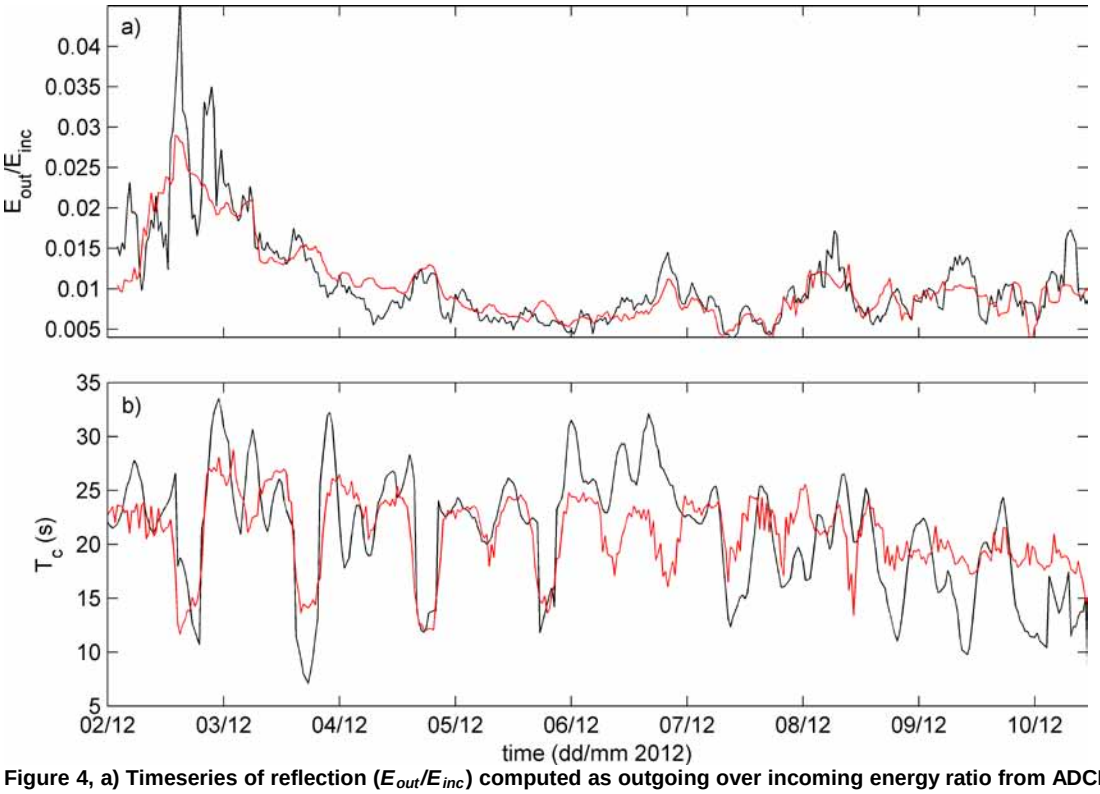

Figure 4, a) Timeseries of reflection (E_{out}/E_{inc}) computed as outgoing over incoming energy ratio from ADCP (10-m depth) and b) cut-off period (T_c) of reflected component, estimated as shortest period present in the outgoing component from ADCP measurements. Red lines stand for reconstructed timeseries from multi-linear regression based on waves (H_s, T_p) and swash zone slope parameters.

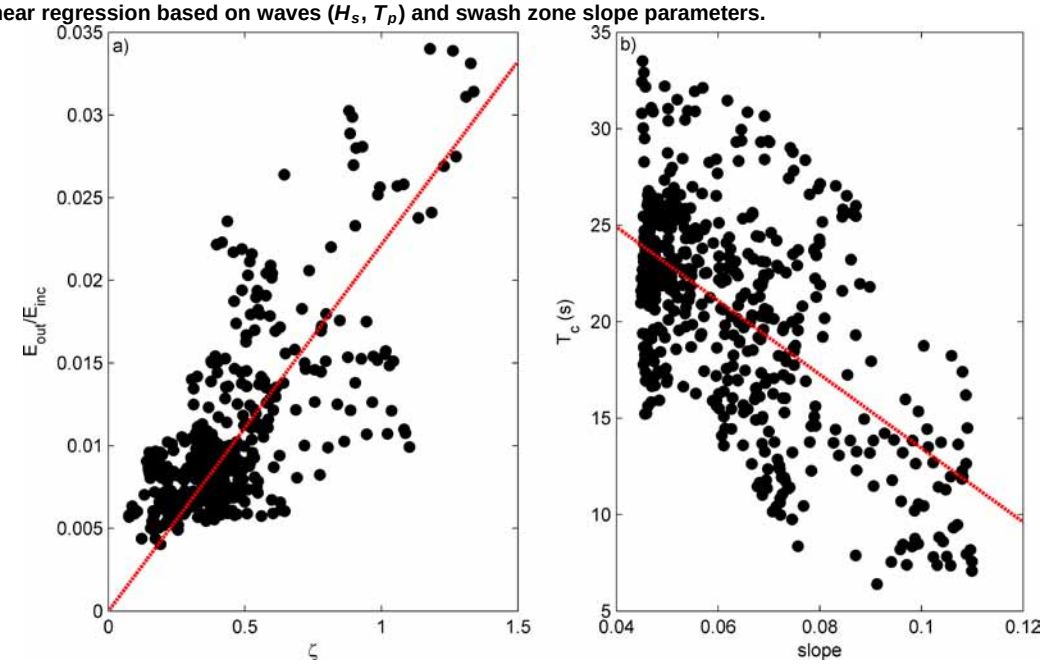

Figure 5, a) Reflection computed as outgoing to incoming energy ratio (E_{out}/E_{inc}), as function of Iribarren number *ξ*. Red dashed line is linear regression (R^2=0.43, reflection=*0.002*ξ*). b) Cut-off period (shortest period in outgoing component) as a function of swash zone slope. Red dashed line is the linear regression (R^2=0.35, *Tc=32-191sl*).

Swash-by-swash measurements using video poles

A new swash and inner surf zone measurement technique is introduced here. This technique is extensively described in Ibaceta et al., (2014, this issue) and only pertinent aspects are described here.

The technique is based on video optical full HD measurement (Fig. 2.b) of a series of vertical poles (2-m, metallic painted) deployed along a cross-shore transect. Image timestacks are generated for each of the poles and image processing based on the colourband difference for sand, water, and pole pixels make possible the extraction of the pixel corresponding to the water surface or bed elevation. This elevation in pixels is converted into real world coordinates, knowing the location (X,Y,Z) of the pole together with the pixel resolution along the poles ($O(10^{-3})$ m). Fig. 6 shows an illustration of the measurement technique for 6 poles deployed (~every 4 m) during the 2012 Mataquito experiment which enables the propagation and transformation of waves in the inner surf and swash zones to be measured. Interestingly, bore merging events can be seen.

Fig. 7.a shows a time series of water surface and bed evolution over a 130 min period when synchronized co-located (~2-3 m) LIDAR measurements are available. Figs. 7.b and 7.c are zoomed in on individual sequences to better understand differences between video and LIDAR measurements. Overall, a good agreement (R^2=0.82) is found between the two techniques, both for bed and surface elevation. A 3 cm RMS difference is found, mainly localized in bore fronts. Video data presents less high frequency noise than LIDAR which tends to underestimate wave front height and non-turbulent backwash slope or even miss small swash events, though some differences might be attributed to the simple fact that the instruments were not exactly at the same location and exposed to a perfectly alongshore-uniform forcing. However, LIDAR presents a much better horizontal resolution (cm) compared to video (typically, ~1m-5m) that is limited by the number of poles deployed.

As a preliminary result of the use of the video technique, incoming and outgoing swash components are separated in order to identify the mechanisms at the origin of the reflection and low-pass filtering of the incoming waves. This is done using the recently developed Radon Transform method (Almar et al., 2014) on cross-shore spatio-temporal data format constructed from 10 poles. Fig. 8 shows results of the separation procedure. While short gravity waves are dominant in the incoming timeseries, they are no longer present in the outgoing timeseries (Fig. 8.a). This is thought to be associated with the non-linear wave transformation in the uprush with swash bore merging (observed in Fig. 6) from long-short waves interactions, but also to the fact that only low frequency waves, lower than the cut-off frequency, are able to reflect in the swash. Uprush and backswash elevation spectra in Fig. 8.b confirm this with an incoming component dominated by gravity wave energy and an outgoing component dominated by infragravity energy. More research is needed to better understand if, and by how much energy at a higher frequency than the cut-off frequency is filtered out by turbulence and friction in the swash, and if the predominant mechanism is associated to frequency transfer from gravity swash to infragravity. It can be hypothesized that these mechanisms co-exist and their relative contribution depends on swash vertical acceleration and bed slope (Brochini and Baldock, 2008). A research effort is also required to better understand the transition from backswash to outgoing wave train in the surf zone.

Figure 6, Video-pole technique illustration for Mataquito 2012 experiment. (up) cross-shore timestack showing the location of the 6 poles (yellow lines) within the swash zone. Lower panels show the vertical timestacks generated along the poles that allow monitoring the propagation of the waves and their deformation while they propagate to the shore. Vertical and temporal resolutions are ~0.001 m and 0.04 s, respectively.

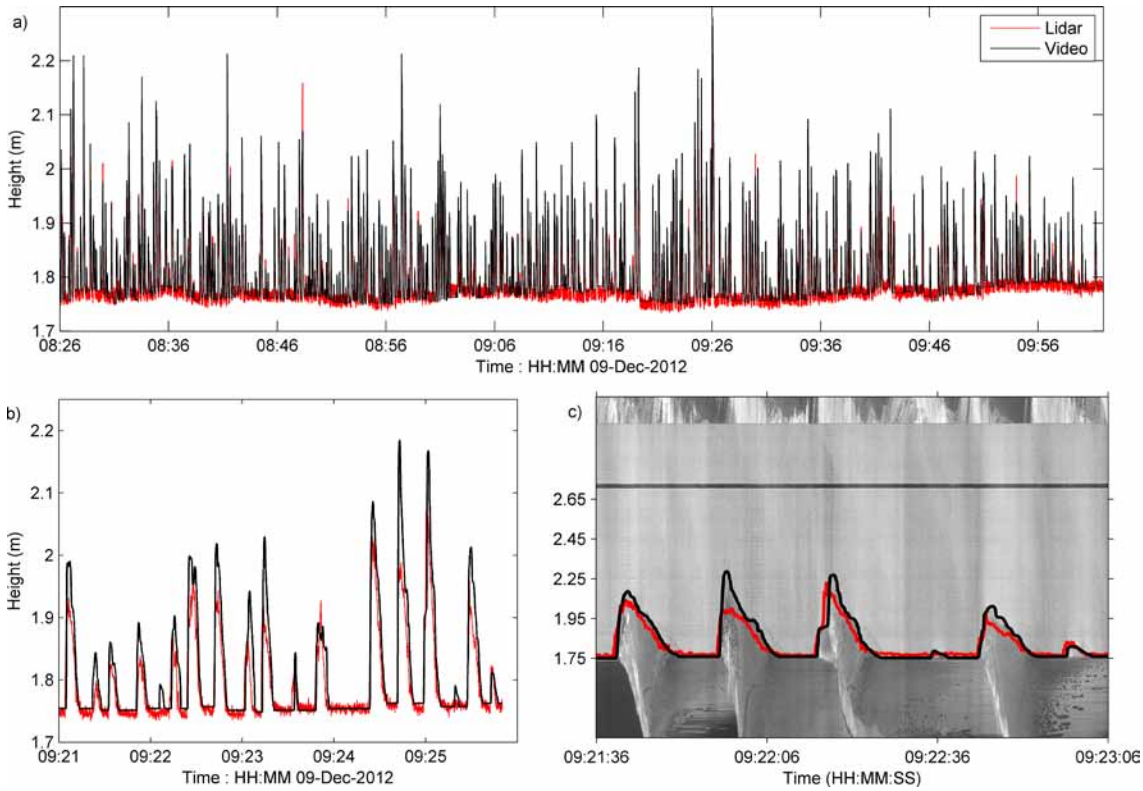

Figure 7, Comparison of video-poles (black) and LIDAR (red) estimated surface and bed elevations over a 130 min period, on Dec. 10 during the Mataquito 2012 experiment. Black line is video and red is LIDAR.

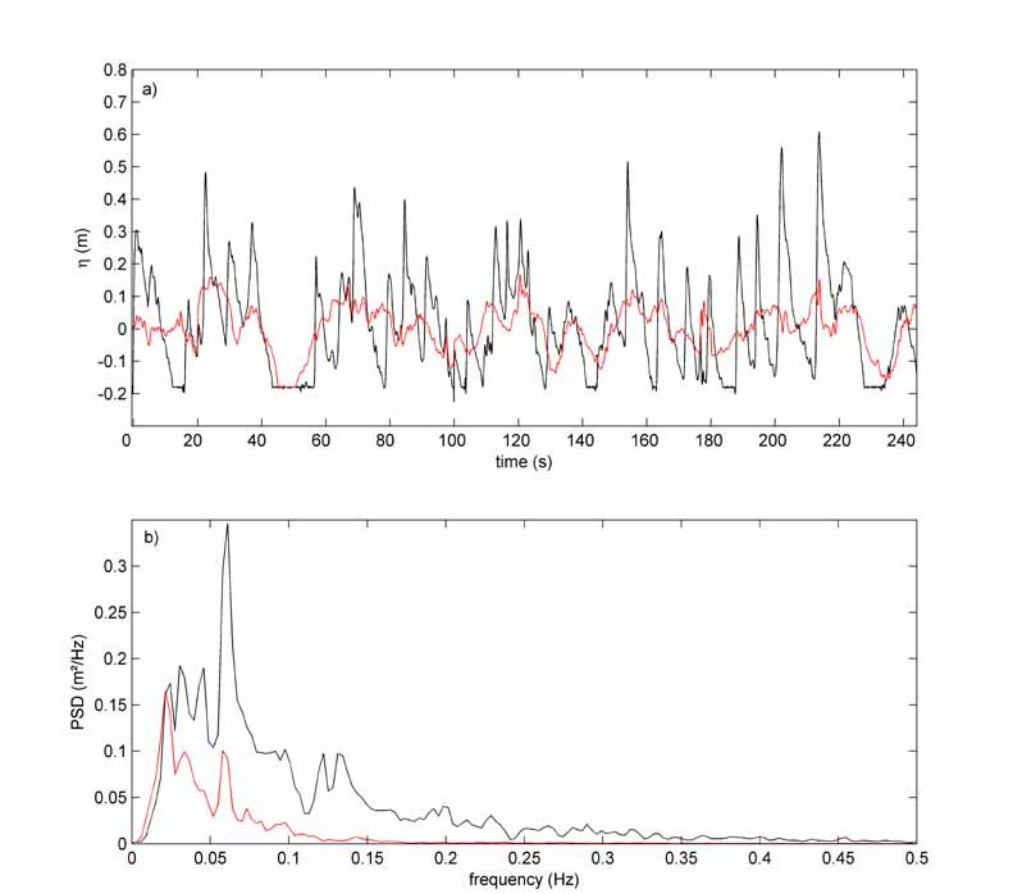

Figure 8, Video-poles derived swash incoming (black) and outgoing (red) a) elevation timeseries and b) energy spectra during Mataquito experiment on Dec. 10 2012, high tide. Incoming and outgoing components are dominated by gravity and infragravity band, respectively

CONCLUSIONS

This paper presents the first large coastal experiment conducted in Chile, at Mataquito, Maule Region, 400 km South West of Santiago de Chile. Wave conditions were very energetic, with Hs in the range 1-4 m, peak wave periods up to 18 s, weak oblique incidence, and a contrasted gently to intermediate sloping beach, which corresponds to mostly dissipative conditions. ADCP, daily beach survey and swash-zone measurements, made possible the estimation of energy reflection and the characterization of outgoing spectrum.

We show that the energy reflection can be well reconstructed (R^2=0.74) from wave parameters and the swash zone slope which have equivalent contribution (~50%). Reflections can be quantified based on the swash-slope based Iribarren number (R^2=0.43) which compares wave steepness and bed slope. The swash acts as a low-frequency filter on the reflected component, the cut-off period was extracted and estimated through a multi-linear reconstruction based again on wave and swash zone slope parameters. This showed a good agreement (R^2=0.48) with swash zone slope having a predominant role (72 %). It was found that swash zone slope is well correlated (R^2=0.35) with cut-off period. These results demonstrate the key role played by the swash dynamics in wave reflection.

To further examine the swash reflection mechanism, a new method for measuring swash hydro-morphodynamics was developed and is introduced in this paper. This low cost technique based on full HD (vertical resolution~0.001 m, temporal resolution 0.04 s) video-poles is described and validated with synchronized co-located LIDAR measurements. A good agreement is found (R^2=0.82, RMS=0.03 m) between the two instruments while the video shows less high frequency noise with a good capture of non-turbulent backwash slopes and small swash events. However, the LIDAR has a much better spatial resolution than the video-pole technique (~0.01 m<<1-5 m) and is less demanding to process. Using the

video-pole technique and the recently developed Radon Transform method for separating incoming from outgoing components, it was found that the uprush and backswash are dominated by gravity and infragravity frequencies, respectively. This suggests the dissipation of shortest waves and/or a non-linear frequency transfer to lower frequency, which clearly shows the low-pass filtering effect in the swash. More investigation of the swash hydro and morphodynamics is needed, moving toward a swash-by-swash approach, to further link swash dynamics to bulk reflection parameters observed offshore. For instance, a research effort is ongoing to estimate individual reflection and impact on bed profile, closely linked to a dynamic definition of the shoreface equilibrium slope (see Anthony et al., 1998).

ACKNOWLEDGMENTS

This work has been funded by the Chilean National Science and technology Committee CONICYT through the Fondecyt project N°1120878. Mauricio Villagran has been supported by CONICYT through a PhD scholarship. The CONICYT/FONDAP/15110017 program is also acknowledged. RA funded by french EC2CO and LEFE INSU/CNRS projects. RI funded by CNRS internship grant.

REFERENCES

Almar, R., Cienfuegos, R., Gonzalez, E., Catalan, P.A., Michallet, H., Bonneton, P., Castelle, B., Suarez, L., 2012. Barred-beach morphological control on infragravity motion, *International Conference on Coastal Engineering*, Santander, Spain, 2-6 July 2012

Anthony,E.J.,1998. Sediment-wave parametric characterization of beaches. Journal of Coastal Research,14(1), 347-352. Royal Palm Beach (Florida), ISSN0749-0208

Battjes, J.A., 1974. Surf similarity. *Proceedings of the 14th International Conference of Coastal Engineering (American Society of Civil Engineers)*, pp.466-480

Blenkinsopp C., M. Mole, I. Turner, W. Peirson. 2010. Measurements of time-varying free-surface profile across the swash zone obtained using an industrial LIDAR. *Coastal Engineering*, 57, 1059-1065

Brocchini M,, and T. Baldock. 2008. Recent advances in modeling swash zone dynamics: Influences of surf-swash interaction on nearshore hydrodynamics and morphodynamics. *Reviews of Geophysics*, 46, No. 3.RG3003

Elgar, S., Herbers, T.H.C. and R. T. Guza, 1994. Reflection of ocean surface gravity waves from a natural beach, J. Physical. Oceanogr., 24(7), 1503-1511

Iribarren, C.R., Nogales, C., 1949. Protection des Ports. *XVIIth International Navigation Congres*, Section II, Communication, 31-80

Ibaceta, R., Almar, R., Lefebvre, J-P., Senoo, T.M., Layrea, W.S., 2014. High frequency monitoring of swash hydromorphodynamics on a reflective beach (Grand Popo, Benin). *International Conference on Coastal Engineering*, Seoul, Corea, June 2014

Holman, R., and Haller, M.C., 2013. Remote sensing of the nearshore, Annual review, Mar Sci. 2013.5:95-113

Miche, R. 1951. Le Pouvoir reflechissant des ouvrages maritimes exposés à l'action de la houle, *Ann. Ponts Chaussees*, 121, 285-319

Miles, J.R, Russell, P.E, 2004 .Dynamics of a reflective beach with a low tide terrace, *Continental Shelf Research*, 24 (11), 1219-1247

Mizuguhi, M., 1984. Swash on a natural beach. *Coastal Engineering Proceedings*, 19. 2156-1028

Sutherland, J., and T. O'Donoghue, 1998. Characteristics of wave reflection spectra, *J. Waterw. Port Coastal Ocean Eng.*, 124(6), 303-311

Villagran M., Cienfuegos R., Almar R., Gironás J., Catalán P., Camaño C. and Dominguez J.C. 2011. Natural post tsunami recovery of Mataquito river mouth after 2010 Chilean tsunami. *Proc. AGU Fall Meeting Conference* (San Francisco, USA)

Vousdoukas M.I., T. Kirupakaramoorthy, H, Oumeraci, M. de la Torre, F. Wubbold, B. Wagner, S. Schimmels. 2014. The role of combined laser scanning and video techniques in monitoring wave-by-wave swash zone processes, *Coastal Engineering*, 83, 2014, 150-165, ISSN 0378-3839